Mechanically compliant grating reflectors for optomechanics

Utku Kemiktarak, Michael Metcalfe, Mathieu Durand, and John Lawall

Related Articles

Thermal model for an early prototype of concentrating photovoltaic for active solar panel initiative system
J. Renewable Sustainable Energy 4, 011601 (2012)

Four-mode plasmonic structure based on a prism-grating anticrossing bandgap
APL: Org. Electron. Photonics 5, 35 (2012)

Four-mode plasmonic structure based on a prism-grating anticrossing bandgap
Appl. Phys. Lett. 100, 063301 (2012)

Laser and focused ion beam combined machining for micro dies
Rev. Sci. Instrum. 83, 02B901 (2012)

Beam-scanning planar lens based on graphene
Appl. Phys. Lett. 100, 051903 (2012)

Additional information on Appl. Phys. Lett.

Mechanically compliant grating reflectors for optomechanics

Utku Kemiktarak,[1,2,a)] Michael Metcalfe,[1,2] Mathieu Durand,[1] and John Lawall[1,b)]
[1]*National Institute of Standards and Technology, 100 Bureau Drive, Gaithersburg, Maryland 20899, USA*
[2]*Joint Quantum Institute, University of Maryland, College Park, Maryland 20742, USA*

We demonstrate micromechanical reflectors with a reflectivity as large as 99.4% and a mechanical quality factor Q as large as 7.8×10^5 for optomechanical applications. The reflectors are silicon nitride membranes patterned with sub-wavelength grating structures, obviating the need for the many dielectric layers used in conventional mirrors. We have employed the reflectors in the construction of a Fabry-Perot cavity with a finesse as high as $F = 1200$, and used the optical response to probe the mechanical properties of the membrane. © *2012 American Institute of Physics*. [doi:10.1063/1.3684248]

Optical Fabry-Perot cavities employing mechanically compliant mirrors have been the subject of intense recent interest for their utility in quantum-limited position measurements,[1] creating nonclassical states of the optical cavity field and mirror,[2,3] and attempting to optically cool fabricated mesoscopic systems into the quantum regime.[4–7] The optical cavity provides a mean to interrogate the dynamics of a mechanical resonator with extremely high sensitivity, while simultaneously providing a large circulating optical power whose radiation pressure can be employed to alter the mechanics.

The ideal optomechanical element for such work combines low mass, high mechanical quality factor Q, and near-unity reflectivity. A small mass confers a large mechanical zero-point motion, which is directly proportional to the optomechanical coupling,[2] closely related to the standard quantum limit for continuous position detection,[1] and of particular relevance to experiments aimed at observing superposition states of the mirror.[3] A high mechanical Q is desirable to minimize thermal noise in position detection.[1] In addition, optical cooling can reduce the mean number of mechanical quanta from an initial value of $\langle n \rangle = k_B T/(h\nu_m)$ by at most a factor of the quality factor Q of the resonator.[6] Finally, high mirror reflectivity is essential to achieve the high cavity finesse required for sensitive position detection, high circulating optical power, and efficient optical cooling.[8]

The majority of the mirrors used in micromechanical Fabry-Perot cavities[9] have incorporated a traditional quarter-wave stack reflector, in which alternating layers of dielectric materials with different refractive indices are deposited. The mirrors typically employ 16-40 layers and have a thickness in the range of $3.6\,\mu m$–$9\,\mu m$. Mechanical resonators exhibiting room-temperature quality factors in the range of $Q = 1000$–9000 have been fabricated directly out of the dielectric stack itself;[10–12] a discussion of the tradeoffs involved with specific dielectric materials is given by Cole.[11] Somewhat higher values of Q, up to $Q = 15\,000$, have been realized with a silicon substrate coated with such a stack.[4] Substantially, higher values of Q, up to $Q = 250\,000$ at room

temperature, have been obtained by using a silicon mechanical resonator to support a smaller reflecting element.[1,9]

In this work, we demonstrate a micromechanical reflector with an unprecedented combination of high reflectivity, high mechanical Q, and low mass per unit area, by taking an altogether different approach. In a dielectric slab patterned as a diffraction grating with a period smaller than the wavelength of the incident light, only zero-order diffraction is allowed. With appropriate design, the transmitted beam can be made arbitrarily small, corresponding to near-unity reflection.[13–17] Recently, devices employing sub-wavelength grating structures as reflectors have been demonstrated inside active vertical-cavity surface-emitting laser (VCSEL)[18] and passive[19] optical resonators. Here, we start with a silicon nitride membrane with a reflectivity of $R = 27\%$, and by removing material so as to pattern it as a grating, we simultaneously reduce its mass and endow it with a reflectivity exceeding 99.4%. We use the patterned membrane as the end mirror in a passive optical cavity and demonstrate an optical finesse $F > 1000$ and room-temperature mechanical quality factors as high as $Q = 7.8 \times 10^5$. The mass per unit area $(7 \times 10^{-4}\,\text{kg m}^{-2})$ of these reflectors is more than an order of magnitude smaller than that of a conventional mirror with the same reflectivity, and the mechanical quality factor is two orders of magnitude higher.

The design of our silicon nitride grating reflectors started with simulation based on 2D rigorous coupled wave analysis (RCWA).[20,21] Early fabrication attempts revealed sloped sidewalls, as shown in Fig. 1(a), which are included in the RCWA calculations. The thicknesses of the silicon nitride film and finger width were chosen in an attempt to make two high-reflectivity modes of the grating coincide,[16] in order to make the region of high reflectivity less sensitive to imperfections in fabrication.

We initiate membrane fabrication by coating silicon wafers with low stress silicon nitride on both sides in a low-pressure chemical vapor deposition system. We then etch out a photolithographically defined patch of silicon nitride from the back surface of the wafer using reactive ion etching (RIE) and, subsequently, etch the exposed silicon in KOH to form a silicon nitride membrane. We pattern the individual membranes with grating structures by means of electron
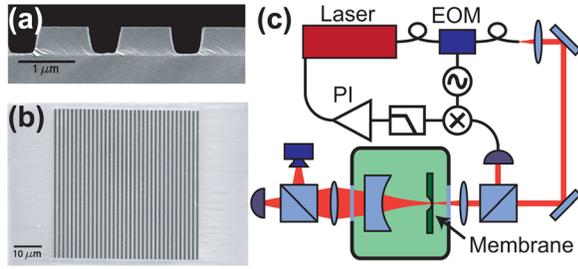

FIG. 1. (Color online) (a) Side view of silicon nitride grating structure revealing sloped sidewalls resulting from the etching process. The substrate is not present in the final devices. (b) One of 81 grating patterns on the membrane, 50 μm on a side. (c) The membrane containing the grating structures is used as one mirror of a Fabry-Perot cavity constructed in vacuum. The laser can be locked to a cavity resonance with a PI (proportional/integral) controller.

beam lithography and a subsequent RIE step, in which the electron beam resist is used as a mask. The membrane used in this work has dimensions of $1.2\,\text{mm} \times 1.2\,\text{mm} \times 470\,\text{nm}$ and is patterned with 81 different grating structures, each $50\,\mu\text{m}$ on a side; one such structure is shown in Fig. 1(b). There is a $50\,\mu\text{m}$ separation between grating patterns, and each grating has a slightly different period and finger width. All of the results in this paper employ a grating located on a diagonal of the membrane, $242\,\mu\text{m}$ from the membrane center, with a period of $1410\,\text{nm}$ and a mean finger width of $660\,\text{nm}$.

In order to characterize the grating reflectors, we constructed a setup allowing an individual grating to be one mirror of a macroscopic Fabry-Perot cavity in vacuum, as shown in Fig. 1(c). The other cavity mirror is a standard curved dielectric mirror with a radius of curvature $R = 25\,\text{mm}$ and reflectivity better than 99.97% over the wavelength range of $1.5\,\mu\text{m}$-$1.6\,\mu\text{m}$. We use a cavity length L_{cav} close to the limit of the stability region given by $L_{cav} < R$,[22] where the waist of the optical mode diminishes rapidly with cavity length. Correspondingly, the cavity free spectral range *FSR* is approximately 6 GHz. An electro-optic modulator (EOM) is used to derive a Pound-Drever-Hall (PDH) error signal.

The optical response of a cavity employing a particular grating is obtained by sweeping the laser frequency over a cavity resonance while monitoring the cavity transmission and reflection. Fig. 2 shows the finesse $F = FSR/\delta\nu_{cav}$ measured

over a wavelength range of 1500 nm–1600 nm, where the cavity FWHM $\delta\nu_{cav}$ is obtained from Lorentzian fits to the transmission. The inset shows the PDH signal at a wavelength of 1560 nm; the width (peak-valley) of the steep central section is approximately equal to $\delta\nu_{cav}$. The finesse varies substantially, with maxima at 1500 nm ($F = 1060 \pm 25$) and 1575 nm ($F = 1200 \pm 120$). The finesse of a low-loss cavity is related to the mirror reflectivities R_i by[23]

$$F = \frac{2\pi}{(1 - R_1) + (1 - R_2)}. \quad (1)$$

A lower bound for the reflection R_1 is thus provided by $R_1 \geq 1 - 2\pi/F$ and yields a value of $R_1 \geq 99.4\%$ at 1575 nm. By comparison, a quarter-wave stack employing conventional dielectrics would need 16-34 dielectric layers to achieve a reflectivity of $R = 99.4\%$, would be 7-10 times thicker, and have 16-31 times the mass per unit area.

The RCWA simulations for this grating show $99.57\% \leq R_1 \leq 99.87\%$ over the wavelength range of Fig. 2, although the result is very sensitive to the parameters; taking a membrane thickness of 465 nm rather than 470 nm changes the lower limit to 99.1%. In addition, the theoretical wavelength dependence is quite different from that measured. We attribute the discrepancy largely to fabrication imperfections, a conclusion that is supported by our observation of large variations in the reflectivity of the gratings patterned on the membrane.

We next describe the mechanical characteristics of the grating reflectors. To this end, we lock a laser with a wavelength of 1560 nm to the cavity with a bandwidth of approximately 12 kHz by means of the PDH signal shown in Fig. 2. Analysis of the rapid ($>$12 kHz) variations in the PDH signal by means of a rf spectrum analyzer reveals hundreds of well-resolved spectral lines in the frequency range of 130 kHz to several MHz. The normal mode frequencies $\nu_{m,n}$ of a uniform square membrane of side a, tensile stress Σ, and density ρ are given by[24]

$$\nu_{m,n}^2 = \frac{\Sigma}{4\rho a^2}(m^2 + n^2), \quad (2)$$

where m and n are positive integers. Fig. 3(a) shows an identification of the eight lowest-frequency modes according to
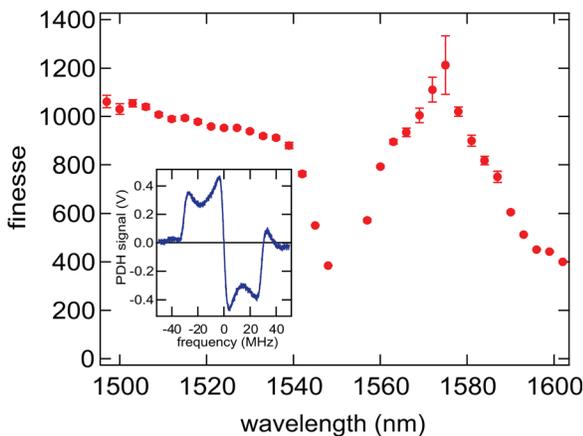

FIG. 2. (Color online) Finesse vs wavelength of cavity in Fig. 1(c). Inset: PDH signal (1 MHz bandwidth) used to lock laser to cavity and transduce mechanical motion.
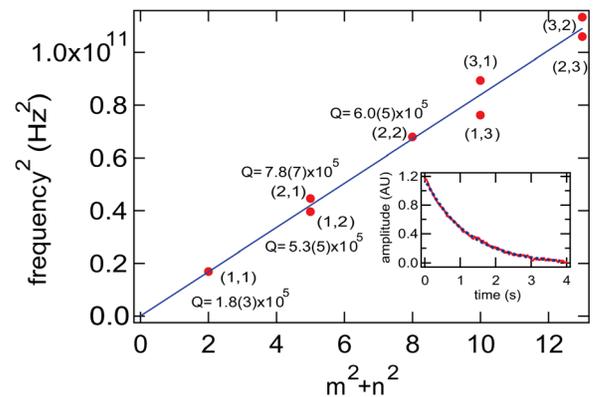

FIG. 3. (Color online) Identification of the eight lowest-frequency mechanical modes, along with mechanical quality factors Q for four modes. Inset: Mechanical ringdown of (2,1) mode at 211 kHz has a time constant of $\tau = 1.18\,\text{s}$, corresponding to a mechanical quality factor of $Q = 7.8 \times 10^5$.

Eq. (2). Clearly, the degeneracy of modes (m,n) with the same sum $m^2 + n^2$ is broken, a fact readily attributable to the asymmetric stress imposed by patterning the membranes with gratings. The amplitude of the response is found to decrease substantially at frequencies above 3 MHz; this is easily understood, as the distance between antinodes[24] is then smaller than the size of the optical spot on the grating.

The rf spectrum analyzer does not have the resolution necessary to measure the intrinsic linewidths of the individual mechanical modes, so for this purpose we turn to a time-domain approach. The membrane is driven at one of its natural frequencies by means of radiation pressure from an intensity-modulated auxiliary laser, and after extinguishing the excitation, the mechanical ringdown is measured with a resonant PDH probe. In this case, the PDH response is demodulated at the mechanical frequency with a lock-in amplifier, and the oscillation amplitude is recorded as a function of time. A typical ringdown measurement, taken on the (2,1) mode with a frequency of 211 kHz, is shown in the inset to Fig. 3. The decay is exponential with a time constant of $\tau = 1.18 \pm 0.11$ s, corresponding to a mechanical quality factor of $Q = \pi\nu_{2,1}\tau = 780\,000 \pm 75\,000$. We have measured in this way the mechanical quality factors $Q_{m,n}$ of the first four modes, which are given in Fig. 3(b) and range from $180\,000$ to $780\,000$. The uncertainties given represent the standard deviation in 20 repeated measurements of τ. Over periods of weeks, or if the sample is removed and repositioned, the quality factors may vary by more than the uncertainties given in the figure.

RCWA simulations including dielectric absorption indicate that reflectivity exceeding 99.96% over a wavelength range of 60 nm should be achievable with structures such as ours employing stoichiometric silicon nitride;[6] the peak finesse would exceed $180\,000$. We believe that fabrication imperfections and associated scattering losses are currently the primary limitations to our device performance, and we are currently studying these matters. In addition to their utility in conventional Fabry-Perot cavities, such highly reflective membranes should be of considerable interest in "membrane in a cavity" experiments as well,[5,6] which to date have employed membranes with reflectivities below 20%.

[1]I. Tittonen, G. Breitenbach, T. Kalkbrenner, T. Müller, R. Conradt, S. Schiller, E. Steinsland, N. Blanc, and N. F. de Rooij, Phys. Rev. A **59**, 1038 (1999).

[2]S. Bose, K. Jacobs, and P. L. Knight, Phys. Rev. A **56**, 4175 (1997).

[3]W. Marshall, C. Simon, R. Penrose, and D. Bouwmeester, Phys. Rev. Lett. **91**, 130401 (2003).

[4]O. Arcizet, P. Cohadon, T. Briant, M. Pinard, A. Heidmann, J. Mackowski, C. Michel, L. Pinard, O. Franais, and L. Rousseau, Phys. Rev. Lett. **97**, 133601 (2006).

[5]J. D. Thompson, B. M. Zwickl, A. M. Jayich, F. Marquardt, S. M. Girvin, and J. G. E. Harris, Nature **452**, 72 (2008).

[6]D. Wilson, C. Regal, S. Papp, and H. Kimble, Phys. Rev. Lett. **103**, 207204 (2009).

[7]S. Gröblacher, J. B. Hertzberg, M. R. Vanner, G. D. Cole, S. Gigan, K. C. Schwab, and M. Aspelmeyer, Nat. Phys. **5**, 485 (2009).

[8]T. J. Kippenberg and K. J. Vahala, Opt. Express **15**, 17172 (2007).

[9]D. Kleckner, W. T. M. Irvine, S. S. R. Oemrawsingh, and D. Bouwmeester, Phys. Rev. A **81**, 043814 (2010).

[10]H. R. Böhm, S. Gigan, F. Blaser, A. Zeilinger, M. Aspelmeyer, G. Langer, D. Bäuerle, J. B. Hertzberg, and K. C. Schwab, Appl. Phys. Lett. **89**, 223101 (2006).

[11]G. D. Cole, S. Gröblacher, K. Gugler, S. Gigan, and M. Aspelmeyer, Appl. Phys. Lett. **92**, 261108 (2008).

[12]S. Gröblacher, S. Gigan, H. R. Böhm, A. Zeilinger, and M. Aspelmeyer, EPL **81**, 54003 (2008).

[13]R. Magnusson and S. Wang, Appl. Phys. Lett. **61**, 1022 (1992).

[14]A. Sharon, D. Rosenblatt, and A. A. Friesem, J. Opt. Soc. Am. A **14**, 2985 (1997).

[15]S. Fan and J. D. Joannopoulos, Phys. Rev. B **65**, 235112 (2002).

[16]C. Mateus, M. Huang, Y. Deng, A. Neureuther, and C. Chang-Hasnain, IEEE Photon. Technol. Lett. **16**, 518 (2004).

[17]P. Lalanne, J. P. Hugonin, and P. Chavel, J. Lightwave Technol. **24**, 2442 (2006).

[18]M. C. Huang, Y. Zhou, and C. J. Chang-Hasnain, Nat. Photonics **1**, 119 (2007).

[19]F. Brückner, D. Friedrich, T. Clausnitzer, M. Britzger, O. Burmeister, K. Danzmann, E. Kley, A. Tünnermann, and R. Schnabel, Phys. Rev. Lett. **104**, 163903 (2010).

[20]M. G. Moharam and T. K. Gaylord, J. Opt. Soc. Am. **71**, 811 (1981).

[21]T. Germer, MIST: Modeled integrated scatter tool, version 3.01 (available as a free download from NIST, 2008).

[22]H. Kogelnik and T. Li, Proc. IEEE **54**, 1312 (1966).

[23]A. Siegman, *Lasers* (University Science Books, Sausalito, 1986).

[24]S. Timoshenko, *Vibration Problems in Engineering* (D. Van Nostrand Company, New York, 1937).